Biophysical Journal Volume 75 June 1999 3044–3057

Hydrodynamic Properties of Rigid Particles: Comparison of Different Modeling and Computational Procedures

Beatriz Carrasco and José García de la Torre
Departamento de Química Física, Facultad de Química, Universidad de Murcia, 30071 Murcia, Spain

ABSTRACT The hydrodynamic properties of rigid particles are calculated from models composed of spherical elements (beads) using theories developed by Kirkwood, Bloomfield, and their coworkers. Bead models have usually been built in such a way that the beads fill the volume occupied by the particles. Sometimes the beads are few and of varying sizes (bead models in the strict sense), and other times there are many small beads (filling models). Because hydrodynamic friction takes place at the molecular surface, another possibility is to use shell models, as originally proposed by Bloomfield. In this work, we have developed procedures to build models of the various kinds, and we describe the theory and methods for calculating their hydrodynamic properties, including approximate methods that may be needed to treat models with a very large number of elements. By combining the various possibilities of model building and hydrodynamic calculation, several strategies can be designed. We have made a quantitative comparison of the performance of the various strategies by applying them to some test cases, for which the properties are known a priori. We provide guidelines and computational tools for bead modeling.

INTRODUCTION

Because of the great number and variety of intramolecular interactions that exist, biological macromolecules frequently have strongly preferred, practically unique, conformations. As a consequence, in solution, they behave as rigid particles with a well-defined, specific shape. Simple geometric models, such as spheres, ellipsoids, or cylinders can, in some cases, be used to describe the solution properties, when the overall shape is almost symmetric and one accepts a low-resolution description. However, there are many situations in which simple models are inadequate, and others in which one wishes to study fine structural details.

The problem of predicting the hydrodynamic properties (sedimentation and diffusion coefficients, relaxation times, intrinsic viscosity) of rigid macromolecules or particles of arbitrarily complex shape was faced in the pioneering works of Bloomfield et al. (1967a,b). These authors worked within the framework of the Kirkwood–Riseman theory of macromolecular hydrodynamics (Kirkwood, 1954; Riseman and Kirkwood, 1956), which had been initially applied to very simple models of identical elements (Riseman and Kirkwood, 1950), and devised procedures for calculating the properties for models composed of equal or unequal spherical elements (beads). Some approximations contained in the early bead model treatments (mainly related to the hydrodynamic interaction effect) that came from the original Kirkwood–Riseman theories were removed in subsequent works (McCammon, 1976; García de la Torre and Bloomfield, 1977a,b, 1978; Nakajima and Wada, 1977; Swanson et al., 1978). In these studies, the nonpointlike nature of the beads was accounted for in the description of hydrodynamic interactions by means of modified-Oseen tensors (Rotne and Prager, 1969; Yamakawa, 1970; García de la Torre and Bloomfield, 1977a), whereas the total frictional forces at each element, from which the properties are computed, were assumed to act at the bead centers. Such a situation is unimportant for models with many small beads, but has a noticeable effect when bead size is close to the overall size of the particle (García de la Torre and Bloomfield, 1978; Wilson and Bloomfield, 1979). This deficiency was corrected in later works (García de la Torre and Rodes, 1983; García de la Torre, 1989; García de la Torre and Carrasco, 1998). Some reviews on theory and applications of rigid bead models are available (Teller et al., 1979; García de la Torre and Bloomfield, 1981; García de la Torre, 1981, 1989, 1992).

Different points of view can be adopted in the construction of bead models for a given particle. In a straightforward approach, one would fill the particle with spherical elements, the only requirement being that the size and shape of the resulting model should be as close as possible to that of the particle. Small, finely shaped details can be properly modeled if one uses a great number of beads of varying size. As will be shown below, this approach works well enough when the hydrodynamic treatment of the model rigorously describes the hydrodynamic interactions. Another alternative for bead modeling is the Bloomfield shell-model approach. As hydrodynamic resistance takes place on the surface of the particle, Bloomfield et al. (1967a) and Filson and Bloomfield (1967) proposed modeling the particle as a shell of small, identical beads. The calculated properties should converge to the exact values as the bead size is decreased, with a subsequent increase in the number of beads, N.

In the rigorous bead-model treatments, the frictional forces are obtained as the solutions of systems of $3N$ linear

Received for publication 4 December 1998 and in final form 29 March 1999.

Address reprint requests to Dr. José García de la Torre, Departamento de Química Física, Facultad de Química, Universidad de Murcia, 30071 Murcia, Spain. Tel.: 34-968-307100; Fax: 34-968-364148; E-mail: jgt@fcu.um.es

0006-3495/99/06/3044/14 $2.00

equations. Accordingly, the required computer time is proportional to N^3, and increases greatly with N. This conflicts with the need to use many beads for the reproduction of fine structural details, or for building shell models. In the classical Kirkwood–Riseman theory, approximations in the treatment of hydrodynamic interaction lead to simple equations in which the hydrodynamic properties are computed from double sums over the elements. This requires a number of operations of the order of N^2, so that the computer time needed for high N is much smaller than for the rigorous treatments.

This conflict between the wish for high-resolution or shell models, the computing time required for rigorous calculation, and the errors that approximate calculation will introduce is another motivation of the present study. From the preceeding considerations, it seems important that model building and hydrodynamic treatments should be discussed jointly. Approximate methods may be the most suitable choice for models with many beads, although their performance will depend not only on the shape of the particle (García de la Torre et al., 1983), but also on which kind of bead model is used.

The outline of this paper is as follows. In the next section, we summarize the basic theory of bead modeling, including both the rigorous and the approximate equations (such a summary is helpful because even the latest reviews are now somehow outdated). In the third section, we proceed with the essential aspect of this paper, namely the description and differentiation of the various procedures that can be used for model building: bead, filling, and shell modeling. The combination of the two theoretical approaches, rigorous and approximate, with the various modeling procedures gives rise to a variety of computational strategies. In the next section of this paper, we test the various strategies, applying them to simple model particles, for which almost exact results are already available, including the sphere and ellipsoids of varying axial ratios. We also consider a typical application of this type of modeling, studying properties of oligomeric arrays of globular subunits. The procedures for model building and hydrodynamic computations have been implemented in computer programs that will be of public domain, freely downloaded from our Internet site. These programs are listed and succinctly described in the last sections of this paper.

THEORY AND COMPUTATIONAL PROCEDURES

Basic theory: Rigorous methods

The theoretical foundations of the hydrodynamic calculations necessary for bead models have been described in a series of publications (García de la Torre and Bloomfield, 1977a, 1978, 1981; García de la Torre and Rodes, 1983; García Bernal and García de la Torre, 1980; García de la Torre, 1989). Because a succinct and complete summary of the results can only be found in some specialized publications (García de la Torre, 1989; García de la Torre et al., 1994; Navarro et al., 1995), we present here an up-to-date, compact summary of the theory, at the same time introducing the quantities and notation that will be used in the following sections of this paper.

For a particle of arbitrary shape, the hydrodynamic resistance is expressed by means of a 6×6 resistance or friction tensor, Ξ. Similarly, the Brownian diffusivity is expressed by a 6×6 diffusion matrix, $\mathcal{D}$, which is related to Ξ through the generalized Einstein relationship, $\mathcal{D} = kT\Xi^{-1}$. Both Ξ and $\mathcal{D}$ can be partitioned in 3×3 blocks, which correspond to translation (*tt*), rotation (*rr*) and translation–rotation coupling (*tr*), so that

$$\mathcal{D} = \begin{pmatrix} \mathbf{D}_{tt} & \mathbf{D}_{tr}^{T} \\ \mathbf{D}_{tr} & \mathbf{D}_{rr} \end{pmatrix} = kT \begin{pmatrix} \Xi_{tt} & \Xi_{tr}^{T} \\ \Xi_{tr} & \Xi_{rr} \end{pmatrix}^{-1}. \quad (1)$$

The superscript T indicates transposition. From the *tt* block, the translational diffusion and friction coefficients are given by

$$D_t = \tfrac{1}{3}\mathrm{Tr}(\mathbf{D}_{tt}), \quad (2)$$

$$f_t = kT/D_t, \quad (3)$$

where Tr is the trace of the tensor. Similarly, the five rotational relaxation times, $\tau_k (k = 1, \ldots, 5)$, are calculated from the eigenvalues of the $\mathbf{D}_{rr}$ tensor, that we simply represent as D_1, D_2, and D_3. The reciprocals of the τ_k' values are given by

$$1/\tau_1 = 6D_r - 2\Delta, \quad (4)$$

$$1/\tau_2 = 3(D_r + D_1), \quad (5)$$

$$1/\tau_3 = 3(D_r + D_2), \quad (6)$$

$$1/\tau_4 = 3(D_r + D_3), \quad (7)$$

$$1/\tau_5 = 6D_r + 2\Delta, \quad (8)$$

where

$$D_r = \tfrac{1}{3}(D_1 + D_2 + D_3) \quad (9)$$

and

$$\Delta = (D_1^2 + D_2^2 + D_3^2 - D_1D_2 - D_1D_3 - D_2D_3)^{1/2}. \quad (10)$$

These relaxation times determine the time (or frequency) dependence in dynamic electrooptical or spectroscopic properties, including electric birefringence and dichroism decays, fluorescence anisotropy decay, and nuclear magnetic resonance relaxation. The way in which the τ_i values enter in the calculation of those properties has been described elsewhere (García de la Torre et al., 1997, 1999).

Sometimes, rotational dynamics is characterized in terms of just one relaxation time, τ_0, which is the harmonic mean of the five τ_i values (García de la Torre et al., 1997)

$$\tau_h^{-1} = \frac{1}{5}\sum_{i=1}^{N} \tau_i^{-1}. \quad (11)$$

It can easily be seen that τ_h is related to the trace of $\mathbf{D}_{rr}$,

$$\tau_h = \frac{1}{6D_r} = \frac{f_r}{6kT}, \tag{12}$$

where $D_r = \frac{1}{3}\,\mathrm{Tr}(\mathbf{D}_{rr})$ and $f_r = kT/D_r$.

The 6×6 diffusion tensor $\mathcal{D}$, and particularly the *tt* and *tr* blocks, depend on the origin to which they refer. The proper choice is the so-called center of diffusion, *D* (Harvey and García de la Torre, 1980), which coincides with the symmetry center for a centrosymmetric particle. Otherwise, $\mathcal{D}$ is first calculated at some arbitrary origin, *O*, and then the position vector of *D* with respect to *O* is calculated as

$$\mathbf{r}_{OD} = \begin{pmatrix} x_{OD} \\ y_{OD} \\ z_{OD} \end{pmatrix} = \begin{pmatrix} D_{rr}^{yy} + D_r^{zz} & -D_{rr}^{xy} & -D_{rr}^{xz} \\ -D_{rr}^{xy} & D_{rr}^{xx} + D_r^{zz} & -D_{rr}^{yz} \\ -D_{rr}^{xz} & -D_{rr}^{yz} & D_{rr}^{yy} + D_{rr}^{xx} \end{pmatrix}^{-1} \begin{pmatrix} D_{tr}^{yz} - D_{tr}^{zy} \\ D_{tr}^{zx} - D_{tr}^{xz} \\ D_{tr}^{xy} - D_{tr}^{yx} \end{pmatrix}, \tag{13}$$

and finally the blocks of $\mathcal{D}$ are recalculated at *D*. For the *tt* block, the transformation is

$$\mathbf{D}_{tt,D} = \mathbf{D}_{tt,O} - \mathbf{U}_{OD} \cdot \mathbf{D}_{rr} \cdot \mathbf{U}_{OD} + \mathbf{D}_{tr}^{T} \cdot \mathbf{U}_{OD} - \mathbf{U}_{OD} \cdot \mathbf{D}_{tr}, \tag{14}$$

where

$$U_{OD} = \begin{pmatrix} 0 & -z_{OD} & y_{OD} \\ z_{OD} & 0 & -x_{OD} \\ -y_{OD} & x_{OD} & 0 \end{pmatrix}. \tag{15}$$

The theory of hydrodynamic properties of bead models provides a procedure to calculate the components of Ξ. A key concept in bead model hydrodynamics is the hydrodynamic interaction effect. The frictional force experienced by a bead depends not only on its relative velocity and its friction coefficient, but also on the frictional forces that act at all the other beads. From the Cartesian coordinates and radii of the *N* beads in the model, the 3×3 hydrodynamic interaction tensors between beads *i* and *j*, $\mathbf{T}_{ij}(i, j = 1, \ldots, N)$ are calculated. This tensor was originally formulated by Oseen as

$$\mathbf{T}_{ij} = (8\pi\eta_0 R_{ij})^{-1}(\mathbf{I} + \mathbf{R}_{ij}\mathbf{R}_{ij}/R_{ij}^2), \tag{16}$$

where $\mathbf{I}$ is the unit tensor and $\mathbf{R}_{ij}$ is the distance vector between elements *i* and *j*. In the derivation of Eq. 16, it was implicitly assumed that the size of the elements is much smaller than R_{ij}. Rotne and Prager (1969) and Yamakawa (1970) derived a new expression valid for interacting elements of equal size, which was later generalized by García de la Torre and Bloomfield (1977a) for elements of different radii, σ_i and σ_j,

$$\mathbf{T}_{ij} = (8\pi\eta_0 R_{ij})^{-1}\left(\mathbf{I} + \frac{\mathbf{R}_{ij}\mathbf{R}_{ij}}{R_{ij}^2} + \frac{\sigma_i^2 + \sigma_j^2}{R_{ij}^2}\left(\frac{1}{3}\mathbf{I} - \frac{\mathbf{R}_{ij}\mathbf{R}_{ij}}{R_{ij}^2}\right)\right). \tag{17}$$

This equation is only valid if $R_{ij} \geq \sigma_i + \sigma_j$. Otherwise, beads *i* and *j* overlap and if they have the same radius, σ, the expression for $\mathbf{T}_{ij}$ is (Rotne and Prager, 1969)

$$\mathbf{T}_{ij} = \frac{1}{6\pi\eta_0\sigma}\left(\left(1 - \frac{9}{32}\frac{R_{ij}}{\sigma}\right)\mathbf{I} + \frac{3}{32}\frac{\mathbf{R}_{ij}\mathbf{R}_{ij}}{R_{ij}\sigma}\right). \tag{18}$$

Now we define a $3N \times 3N$ supermatrix $\mathcal{B}$ composed of 3×3 blocks:

$$\mathbf{B}_{ij} = \mathbf{T}_{ij} \quad \text{if} \quad i \neq j, \tag{19}$$

$$\mathbf{B}_{ii} = (1/\zeta_i)\mathbf{I}, \tag{20}$$

where

$$\zeta_i = 6\pi\eta_0\sigma_i \tag{21}$$

is the Stokes' law friction coefficient of bead *i*, with radius σ_i, η_0 being the viscosity of the solvent. This supermatrix is then inverted to obtain a $3N \times 3N$ supermatrix,

$$\mathcal{C} = \mathcal{B}^{-1}, \tag{22}$$

that is partitioned in 3×3 blocks, $\mathbf{C}_{ij}$, which in turn gives the components of Ξ as

$$\Xi_{tt} = \sum_i \sum_j \mathbf{C}_{ij}, \tag{23}$$

$$\Xi_{tr} = \sum_i \sum_j \mathbf{U}_i \cdot \mathbf{C}_{ij}, \tag{24}$$

$$\Xi_{rr}^{uncorr} = \sum_i \sum_j \mathbf{U}_i \cdot \mathbf{C}_{ij} \cdot \mathbf{U}_j \tag{25}$$

where

$$\mathbf{U}_i = \begin{pmatrix} 0 & -z_i & y_i \\ z_i & 0 & -x_i \\ -y_i & x_i & 0 \end{pmatrix}. \tag{26}$$

From the $\mathbf{C}_{ij}$ tensors, the intrinsic viscosity can be calculated directly. First, a particular point that is called the viscosity center has to be located. The procedure is simple, but the corresponding equations are lengthy and the reader is referred to García de la Torre and Bloomfield (1978). Then, the coordinates $r_i'^{\alpha}(\alpha = x, y, z)$ are calculated with that origin, and the intrinsic viscosity is given by:

$$[\eta]^{uncorr} = \frac{N_A}{M\eta_0}\sum_i \sum_j \left(\frac{1}{15}\sum_\alpha r_i'^{\alpha} C_{ij}^{\alpha\alpha} r_j'^{\alpha} + \frac{1}{20}\sum_{\alpha\neq}\sum_\beta r_i'^{\alpha} C_{ij}^{\beta\alpha} r_j'^{\beta} - \frac{1}{30}\sum_{\alpha\neq}\sum_\beta r_i'^{\alpha} C_{ij}^{\alpha\beta} r_j'^{\beta} + \frac{1}{20}\sum_{\alpha\neq}\sum_\beta r_i'^{\alpha} C_{ij}^{\beta\beta} r_j'^{\beta}\right), \tag{27}$$

where N_A is Avogadro's number and M is the molecular weight of the macromolecule.

Summarizing, the computational route is as follows: from the Cartesian coordinates and radii of beads, we calculate the $\mathbf{T}_{ij}$ tensors (Eq. 17) and build the $\mathcal{B}$ supermatrix (Eqs. 19, 20), which is inverted (Eq. 22) to obtain $\mathcal{C}$. The components of Ξ are calculated from Eqs. 23–25. Then, Ξ is inverted to obtain $\mathcal{D}$, which is partitioned into four 3×3 blocks, from which the translational and rotational properties are calculated from Eqs. 2–10.

In Eqs. 25 and 27, for rotation and viscosity, respectively, the subscript uncorr stands for uncorrected, in the sense that the so-called volume corrections are not yet included, and therefore results from them may suffer from the deficiencies mentioned in the Introduction. These corrections will be described below.

The hydrodynamics of the arbitrarily shaped rigid particle simplifies for the case of axisymmetric particles, which is also the case of the test particles used in the numerical calculations that we report later. When referring to the main axes of an axisymmetric particle, the translational and rotational tensors are diagonal. Thus, Ξ_{tt} only has the diagonal components $f_t^{\perp} \equiv f_t^{(x)} = f_t^{(y)}$ and $f_t^{\parallel} = f_t^{(z)}$ where z is the symmetry axis. Similarly, we have components $f_r^{\perp}$ and $f_r^{\parallel}$ for Ξ_{rr}, $D_t^{\perp}$ and $D_t^{\parallel}$ for $\mathbf{D}_{tt}$ and $D_r^{\perp}$ and $D_r^{\parallel}$ for $\mathbf{D}_{rr}$. Individual Einstein relationships, $D = kT/f$, hold for any of these components (for instance $D_r^{\parallel} = kT/f_r^{\parallel}$). At this point, the friction and diffusion tensors refer to the center of diffusion calculated as described above for the general case. In many practical instances, the particle has a center of symmetry with which the hydrodynamic center should coincide. In this case, the Cartesian axes can be centered on it, so that evaluation of the center of diffusion (Eq. 13) and subsequent translation of the hydrodynamic tensors is not necessary. Finally, of the five relaxation times (Eq. 4–8), there are only three distinct values given by

$$\tau_a = (6D_r^{\perp})^{-1} = f_r^{\perp}/(6kT), \tag{28}$$

$$\tau_b = (5D_r^{\perp} + D_r^{\parallel})^{-1} = [kT(5/f_r^{\perp} + 1/f_r^{\parallel})]^{-1}, \tag{29}$$

$$\tau_c = (2D_r^{\perp} + 4D_r^{\parallel})^{-1} = [kT(2/f_r^{\perp} + 4/f_r^{\parallel})]^{-1}, \tag{30}$$

and the harmonic mean relaxation time is given by Eq. 12 with

$$\frac{1}{f_r} = \frac{(2/f_r^{\perp} + 1/f_r^{\parallel})}{3}, \tag{31}$$

and $D_r = (2D_r^{\perp} + D_r^{\parallel})$.

The rotational diffusion of macromolecules is detected by the time or frequency dependence of electrooptic or spectroscopic properties, such as electric birefringence and dichroism, fluorescence anisotropy and nuclear magnetic resonance. The time functions can be calculated by combining the rotational quantities (D_r and the τ_k) and the physical quantities corresponding to each property, as described elsewhere (García de la Torre et al., 1997, 1999).

Basic theory: Approximate methods

Since the pioneering work of Kirkwood, (Kirkwood, 1954; Kirkwood and Riseman, 1948), it has been known that hydrodynamic properties can be calculated by means of approximate, simple formulas that, at the cost of some error in the numerical results, offer the great advantage of having much smaller computational requirements. All these approximate equations involve just a double sum, over pairs of beads, of a simple term, which depends on the interbead distances and the bead friction coefficient or radii.

The paradigmatic case is Kirkwood's formula (Kirkwood, 1954) for f_t (or $D_t = kT/f_t$) modified by Bloomfield et al. (1967a) for unequal beads,

$$f_t = \frac{\sum_{i=1}^{N} \zeta_i}{1 + (6\pi\eta_0 \sum_{i=1}^{N} \zeta_i)^{-1} \sum_{i\neq}^{N} \sum_{j}^{N} \zeta_i \zeta_j r_{ij}^{-1}}. \tag{32}$$

For rotation, similar formulas for individual coefficients (Hearst, 1962) have been generalized to calculate the full rotational friction tensor (García de la Torre et al., 1987). The result is

$$\Xi_{rr}^{uncorr} = (\mathbf{A}_{uncorr}^{-1} + \mathbf{A}_{uncorr}^{-1} \cdot \mathbf{B} \cdot \mathbf{A}_{uncorr})^{-1} \tag{33}$$

or

$$\mathbf{D}_r^{uncorr} = kT(\mathbf{A}_{uncorr}^{-1} + \mathbf{A}_{uncorr}^{-1} \cdot \mathbf{B} \cdot \mathbf{A}_{uncorr}), \tag{34}$$

where

$$\mathbf{A}_{uncorr} = -\sum_{i=1}^{N} \zeta_i \mathbf{U}_i \cdot \mathbf{U}_i, \tag{35}$$

and

$$\mathbf{B} = -\sum_{i\neq}^{N} \sum_{j}^{N} \zeta_i \zeta_j \mathbf{U}_i \cdot \mathbf{T}_{ij} \cdot \mathbf{U}_j, \tag{36}$$

where the $\mathbf{U}_i$ matrices are given by Eq. 26. The bead positions refer to an approximate hydrodynamic center, A, given by

$$\mathbf{r}_{OA} = \sum \zeta_i \mathbf{r}_i \Big/ \sum_i \zeta_i. \tag{37}$$

Finally, for the intrinsic viscosity, we adopt the expression of Tsuda (1970a,b).

$$[\eta]_{uncorr} = \frac{N_A \pi}{M} \left(\sum_i \sigma_i R_i^2 \right) \cdot \left[1 + \frac{1}{\sum_i \sigma_i R_i^2} \frac{3}{4} \left(\sum_{i\neq} \sum_j \sigma_i \sigma_j \left(\frac{R_i R_j \cos \alpha_{ij}}{R_{ij}} + \frac{4(R_i^2 + R_j^2) R_i R_j \cos \alpha_{ij} - R_i^2 R_j^2 (1 + 7\cos^2 \alpha_{ij})}{10 R_{ij}^3} \right) \right) \right]. \tag{38}$$

Further details, such as particular expressions for axisymmetric particles, or a performance analysis for various typical models, are described elsewhere (García de la Torre et al., 1983, 1987).

Volume correction for rotation and intrinsic viscosity

It was soon clear that the rotational friction calculated from Eq. 25 or 33, and the intrinsic viscosities calculated from Eq. 27 or Eq. 38, are in some way erroneous when applied to models in which one or a few spheres have a size close to that of the whole particle. Actually, for a single sphere, these equations give the erroneous results $\Xi_{rr}^{uncorr} = 0$ and $[\eta]_{uncorr} = 0$ instead of the Kirchoff and Einstein expressions. Wilson and Bloomfield (1979) proposed a modeling strategy in which each bead in the model is replaced by a cubic array, and the procedure has been successfully used in other works (García Bernal and García de la Torre, 1981; Allison and McCammon, 1984). The evident drawback is that, as the number of elements increases by a factor of 8, the computing time of the rigorous procedure increases by $8^3 = 512$. This is unimportant for bead models with a few subunits [for instance for oligomeric arrays of spheres (García Bernal and García de la Torre, 1981)] but it may pose a serious problem for other types of model.

With this problem in mind, García de la Torre and Rodes (1983) developed (from rigorous hydrodynamics) a simple, additive correction for the rotational friction tensor, that was successfully tested in various cases. The so-called volume correction for the rotational properties is an additive contribution to the diagonal components of the rotational friction tensor,

$$\Xi_{rr} = \Xi_{rr}^{uncorr} + 6\eta_0 V\mathbf{I}, \tag{39}$$

where $\mathbf{I}$ is the unitary tensor, η_0 is the solvent viscosity and V is the volume of the model, equal to

$$V_m = \frac{4}{3}\pi \sum_{i=1}^{N} \sigma_i^3, \tag{40}$$

where the σ_i are the individual bead radii.

For the intrinsic viscosity, a similar correction is possible. That possibility was hinted at in a preliminary publication (García de la Torre, 1989) and included in the HYDRO computer program (García de la Torre et al., 1994). In a recent work, we have provided the theoretical justification and tested the correction in various instances (García de la Torre and Carrasco, 1998). As in the case of rotational friction, the correction consists of adding a simple term,

$$[\eta] = \frac{5N_A V_m}{2M} + [\eta]_{uncorr}. \tag{41}$$

We recall that V is the total volume of the bead model, understood as the sum of the volumes of all the spheres. This must be kept in mind when using shell-type models (see below), in which the particle's volume is not filled by beads. A frequent situation is that of models composed of identical spheres. In such a case, the volume correction for viscosity reduces to

$$[\eta] = [\eta]_1 + [\eta]_{uncorr}, \tag{42}$$

where $[\eta]_1 = 5N_A V_1/2M_1$ is the intrinsic viscosity of a single bead (monomer) with volume V_1 and molecular mass M_1. This particular result has been reported in previous works (Bianchi and Peterlin, 1968; Yoshizaki et al., 1988; Abe et al., 1991).

TYPES OF MODELING

In a general sense, a bead model is any representation of a particle as an array of spherical frictional elements. In all cases, individual, Stokes-law friction coefficients, ζ_i, are assigned to each element, and the hydrodynamic interaction between them is accounted for by means of the Oseen or modified Oseen tensors.

However, for any given particle, there are different strategies for building the hydrodynamic bead model. Indeed, different modeling methods have been used from the very first works in this field (Bloomfield, 1966; Bloomfield et al., 1967a,b; Bloomfield and Filson, 1968).

We shall refer hereafter to three different classes denoted as *bead model* (in strict sense), *shell model*, and *filling model* (see Figure 1).

Bead model

We shall keep the term bead model, in a strict sense, for a modeling method in which the particle is represented by as few beads as possible, identical or different, and occupying approximately the volume of the particle. The array of beads should have an envelope that resembles the shape of the particle as closely as possible. A schematic illustration in two dimensions is shown in Fig. 1 *A*. Another trivial example is a string of colinear spheres as the bead model of a rod. A classical example of bead modeling is Bloomfield's model for T2 bacteriophage (Bloomfield et al., 1967b) shown in Fig. 2.

Many other examples are described in the literature; one of the earliest examples being Bloomfield's model for a bovine serum albumin (Bloomfield, 1966) or the model for the T-even bacteriophage, in which the massive head is represented by just one large sphere, and the rodlike portions by a string of smaller beads (García de la Torre and Bloomfield, 1977c). When modeling elongated structures, the essential criterion is that the model has the same length and volume as the particle. This criterion is usually followed when modeling rods (Hagerman and Zimm, 1982) and has also been used for the modified ellipsoid model (García de la Torre and Bloomfield, 1977a,b, 1978).

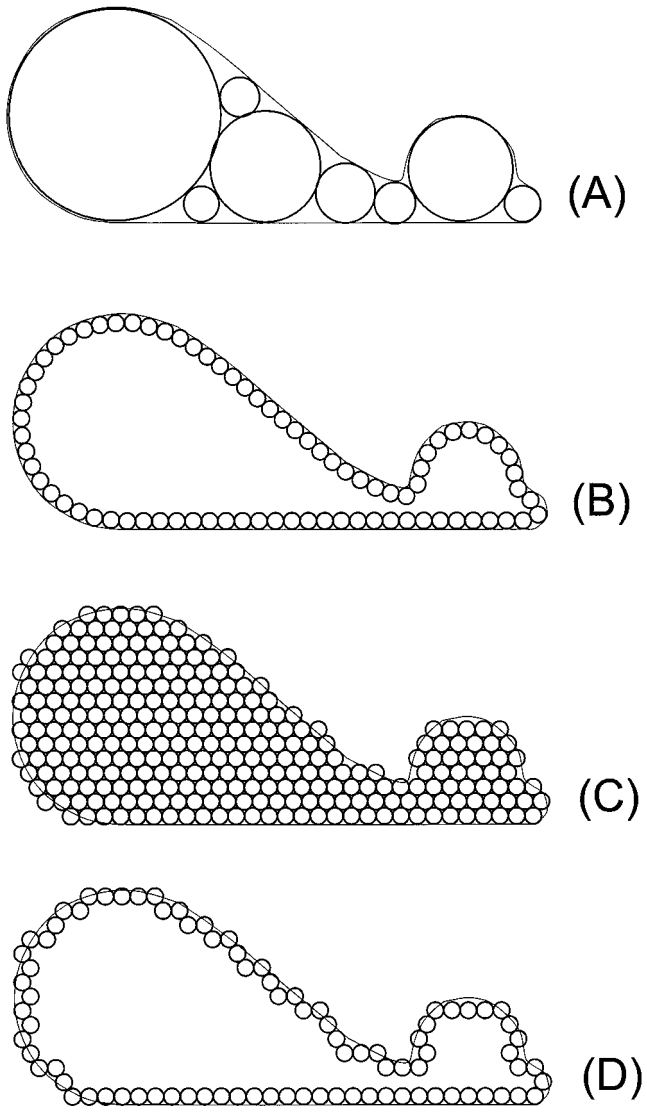

FIGURE 1 Two-dimensional analogies of the various model types. (*A*) A bead model (in strict sense). (*B*) Shell model. (*C*) Filling model. (*D*) Rough-shell model.

The above mentioned strategy of cubic substitution (Wilson and Bloomfield, 1979; García Bernal and García de la Torre, 1981) can be included within the category of bead modeling, in which one, a few, or all the beads can be replaced. For instance, for the T2 model in Fig. 2, it is possible to simply replace the huge bead representing the phage head. In other models, consisting of few beads of similar size, all the beads will be replaced. Such would be the case of the dimeric and oligomeric structures that will be used later in this paper.

As mentioned above, there is an alternative strategy, the cubic substitution, which is intended to remove some of the difficulties involved in rotational and viscosity calculations. In this procedure, each bead is replaced by a cubic array of smaller spheres of a radius such that their total volume is the same as that of the parent sphere.

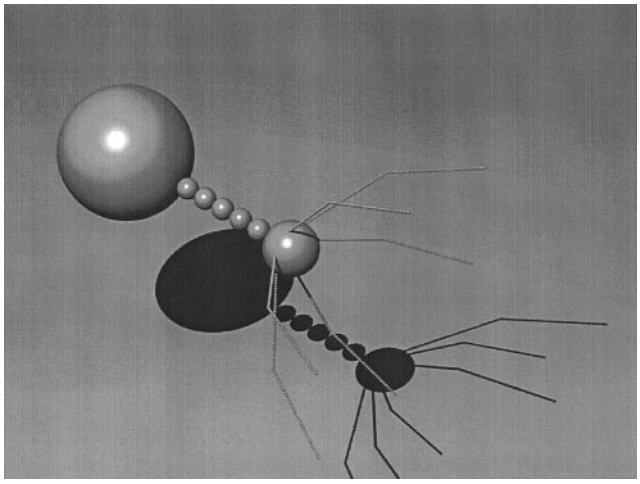

FIGURE 2 Bloomfield's bead model for T2 bacteriophage, as proposed by Bloomfield et al. (1967b).

Shell model

For a compact, solid particle, hydrodynamic friction occurs actually on its surface. In the case of a real macromolecule such as a globular protein, this may indeed be the case, because the interior of the protein is inaccessible to solvent. Even if the macromolecule is somehow porous or permeable to the solvent, the fluid inside it is trapped, moves along with it, and belongs to the hydrodynamic particle. It is therefore the particle's surface that counts.

With this idea in mind, Bloomfield et al. (1967a) and Filson and Bloomfield (1967) proposed the shell model, in which the particle's surface is represented by a shell-like assemblage of many small, identical frictional elements. The bead radius, σ, can be taken such that neighboring beads are tangent (although some minor voids and overlaps are acceptable). The limit of a continuous shell (smooth surface) is approached by increasing the number of elements while decreasing the size, and the properties calculated for the shell will approach the properties of the particle being modeled. Calculations can be made by varying σ, and the results can be extrapolated to the $\sigma \rightarrow 0$, $N \rightarrow \infty$ limit.

Examples of shell modeling were given by Bloomfield et al. for spheres and ellipsoids (Bloomfield et al., 1967a; Filson and Bloomfield, 1967; Bloomfield and Filson, 1968). This type of model was also used by Tirado and García de la Torre for calculating properties of short cylinders with a moderate length-to-diameter ratio (Tirado and García de la Torre, 1979, 1980; Tirado et al., 1984).

A schematic representation of shell modeling is presented in Fig. 1 *B*. Some procedure has to be developed for placing the spherical beads (specifying their coordinates) on the surface, so that each bead is nearly tangent to its neighbors. One possibility is for the beads also to be tangent to the inner face of the surface. Alternatively, beads can be centered on the surface (our choice), or tangent to the outer face; the small differences among these possibilities must vanish in the limit of very small bead size. The modeling

procedure is particularly easy for revolution bodies, like ellipsoids or cylinders, for which beads can be placed at the parallel circumferences defined by planes perpendicular to the main symmetry axis. Thus, by stacking rings of beads of varying ring radius, we can build smooth shell models. An example is presented in Fig. 3 *A*.

It is evident that the finest details of an irregular, arbitrary shape can be modeled if one increases the resolution, as determined by the element radius σ. The adequate computational procedure consists of repeating the calculations for models with decreasing σ, and extrapolating the results to the shell-model limit, $\sigma \rightarrow 0$. However, this substantially increases the computing time necessary for calculating the hydrodynamic properties. The number of elements required to cover the surface area of the particle, S, is given by $N = cS/(4\pi\sigma^2)$, where $c < 1$ is some numerical factor according for the voids between touching spheres. The computer time grows as N^2 or N^3, depending on the hydrodynamic method (approximate or rigorous) used, and it will therefore increase with decreasing σ as σ^{-4} or σ^{-6}, respectively. As an orientation for the reader, we give the following computing times in a Silicon Graphics MIPS R1000 180MHz CPU, for a structure with $N = 500$, about 30 minutes for the rigorous methods and about 2 seconds for the approximate, double-sum methods. The approximate methods are much faster, but, as shown below, they may introduce appreciable errors; the rigorous hydrodynamics requires much larger, but still accessible amounts of CPU time.

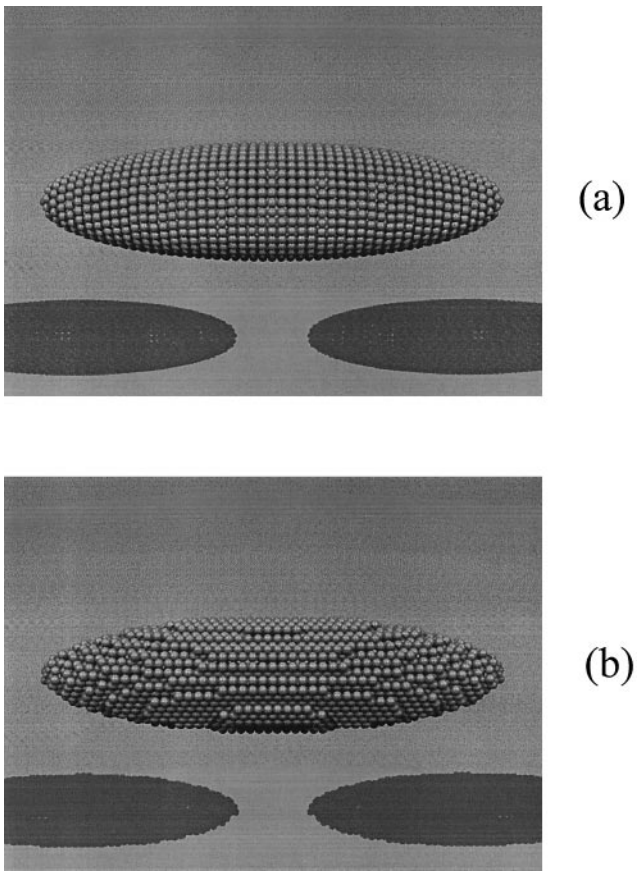

FIGURE 3 Shell models for an ellipsoid with axial ratio $p = 4$. (*A*) Smooth shell. (*B*) Rough shell.

Filling model and rough-shell model

In an alternative modeling method, the volume occupied by the particle can be filled by elements, which is the proper procedure for some properties that depend specifically on the particle volume. Such is the case for the angular dependence of radiation (light or x-ray) scattering from the particle. An evident example is the radius of gyration, that determines the angular dependence at small scattering vectors. In a commonly used procedure for predicting scattering diagrams, the particle is filled with scattering elements and, from their coordinates and size (the same information that is required for hydrodynamics), the scattering structure factor is calculated using the Debye formula (Muller et al., 1983a,b; Muller, 1983; Pavlov and Fedorov, 1983; Pavlov et al., 1986).

The filling model can be programmed as follows. A portion of a regular lattice is spatially superimposed on the particle. The dimensions of such a portion are taken as the maximum dimensions of the particle in three mutually perpendicular directions, thus assuring that the whole particle's volume is covered by the network. An algorithm specifying the shape of the particle is required; the task of which will simply be to decide whether or not a given point in space is within the particle. This is applied to all the nodes in the lattice, and model elements are placed at those nodes that belong to the particle. Here, the elements are beads of radius σ. A simple cubic lattice would suffice, but, for the calculations reported in this paper, we have preferred a hexagonal, closest-packing lattice. A schematic picture of the filling model is presented in Fig. 1 *C*.

As mentioned above, the filling model is, in principle, inefficient for hydrodynamic calculations because it includes internal beads that do not contribute to friction. For a given particle volume, the number of beads needed to fill it is $N = 3qV/(4\pi\sigma^3)$, where $q < 1$ is a numerical factor accounting for the voids between spheres. Thus, the computing time grows dramatically with decreasing σ as σ^{-9} or σ^{-6}, for the rigorous and the double-sum calculations, respectively. Furthermore, we shall describe later the computational deficiencies associated with filling models. However, such models do have some advantages. For example, for particles of complex shape, programming is simpler than with a smooth shell model. In addition, it may be advantageous to use the same model for both scattering and hydrodynamic calculations if the properties of both types are available.

Based on the filling model, an alternative model, which avoids the hydrodynamic problems but which is still compatible with scattering, can be proposed. In such a model, the innermost beads are simply removed, so that we are left with a shell model in which the particle surface is described in a rough manner, with some discontinuities (edges or

corners of the lattice) that will become less important when the resolution is increased by decreasing σ. We shall refer to this as the rough-shell model, which is schematically represented in Fig. 1 *D*. A model of this type for a revolution ellipsoid is displayed in Fig. 3 *B*. At the limit when $\sigma \to 0$, the model converges to the shell model of the smooth surface. The computing time depends on the number of beads or the resolution required, just as it does with the smooth shell model.

The practical implementation of this procedure is extremely simple. A bead is considered internal when it is completely surrounded by other beads; the number of beads that are in touch with it (at a distance equal to 2σ) is maximum, equal to the coordination number of the lattice, which equals 12 for the hexagonal lattice that we use. In the modeling protocol, a filling model is first constructed. Eventually, the radius of gyration and other scattering related properties can be calculated at this stage. Next, the beads that, according to this criterion, are internal are removed to obtain the rough-shell model.

RESULTS AND DISCUSSION

In this section, we use models of the various types, to which we apply both rigorous and approximate hydrodynamic computation. This is done for simple particles whose hydrodynamic properties are perfectly known, and can be calculated from exact, analytical expressions. The performance of the procedures for the different properties can be expressed in terms of the ratio of the calculated property to the exact values, or as the percent deviation,

$$\text{deviation}(\%) = 100\left(\frac{\text{property(calc.)}}{\text{property(exact)}} - 1\right). \quad (43)$$

These deviations are to be judged comparatively to the precision of the experimental methods used to measure the hydrodynamic properties. Experimental errors and numerical uncertainties in final values of the properties depend on a variety of circumstances, but if we say that typical values are, very roughly, of up to 2% for translation (ultracentrifugation and light-scattering), up to 4% for rotation, and up to 8% for intrinsic viscosity, the deviations in the modeling results that would fall below these percentages would be considered as not relevant (different estimates for the typical errors would not change the overall conclusions).

We first consider the simplest case of a spherical particle, and discuss the results in terms of the type of model. Then, we consider ellipsoidal models, which are useful for showing the errors introduced by the approximate methods, which are more noticeable for elongated shapes. We also consider a dimer and some oligomeric structures.

Spherical particles: Shell models versus filling models, and adequacy of the volume correction

An analysis of the results for the spherical model and those for different models using a hydrodynamic approach has a two-fold interest. Apart from the theoretical aspects, the conclusions can be applied to particles that are compact and not too elongated, and particularly to globular proteins.

Smooth shell models for a sphere are easily programmed by stacking rings of beads of varying ring size (in analogy with parallels on the Earth's surface). (See Fig. 3). Filling and rough shell models are extracted from a closest-packing lattice, as described above. For the three models, calculations are carried out using both the rigorous procedures and the approximate formulas summarized above. The calculations are made for a series of decreasing bead diameters, σ, and the results are extrapolated to zero bead size, using linear or, in most cases, quadratic extrapolation. For the rigorous method, the computer time needed restricted the calculation to models with several hundred beads, whereas the double-sum formulas could be evaluated for many thousand beads.

Ratios between the calculated translation friction coefficient of the model and the exact value of a sphere of radius, a, $f_t(\text{exact}) = 6\pi\eta_0 a$, are presented in Fig. 4. It is clear that both smooth and rough shell models give the exact result at the limit of zero bead size. The extrapolated values for the approximate methods are as good as those from the rigorous procedure. For the filling model, the rigorous calculations extrapolate to the correct result, whereas the approximate method fails remarkably in this case.

A similar analysis can be made for the rotational friction coefficient, whose exact value for a sphere is given by $f_r(\text{exact}) = 8\pi\eta_0 a^3 = 6\eta_0 V_p$, where V_p is the sphere's volume. Again, we note that the approximate results extrapolate correctly to the same limit as the rigorous results (see Fig. 5). For rotation, we can choose whether or not to include the volume correction. In Fig. 5 (*top*), one can appreciate the effect of the volume correction for the shell model. For discrete σ, the corrected results are somewhat higher than the uncorrected (the correction is positive). The influence of the volume correction superimposes on the effects of the modeling procedure and finite bead size, and the resulting ratios are more or less close to unity, depending on the case. However, at the shell-model limit, the correction vanishes, and both corrected and uncorrected results converge to the exact value. This is quite simple to understand. If the surface area of the particle, S, is covered by nearly touching beads of radius σ, their number will be $N = cS/(4\pi\sigma^2)$, where c is some numeric constant that accounts for the voids between tangent spheres. The total volume of the N beads will then be $V_m = cS\sigma/3$ (we recall that V_m in Eqs. 37 and 40 is the volume of the model, not that of the particle). Therefore, as the bead size is decreased, i.e., $\sigma \to 0$, we have $V_m \to 0$; in other words, the correction vanishes at the limit of an infinitely thin shell. This argument is not exclusive of the spherical geometry; rather, it can be generalized to particles of arbitrary shape.

In Fig. 5 (*bottom*), we display rotational results for the filling model. It is evident that only the rigorous results, without the volume correction, are adequate. It has already been mentioned that internal beads are hydrodynamically

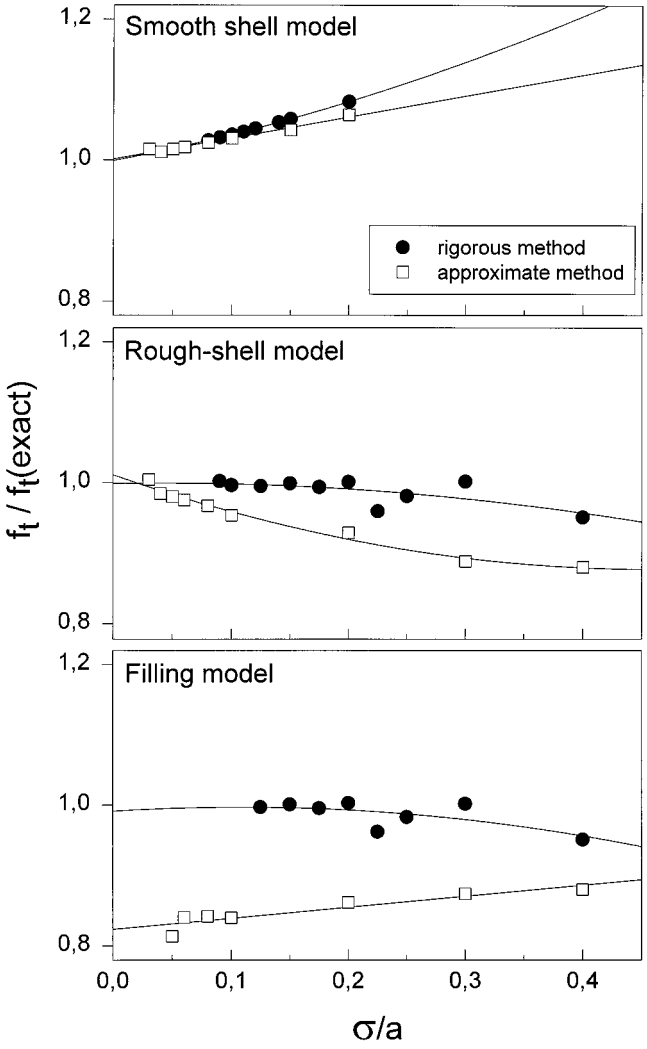

FIGURE 4 Ratios between the calculated translation friction coefficient of the model, f_t, and the exact value of the sphere.

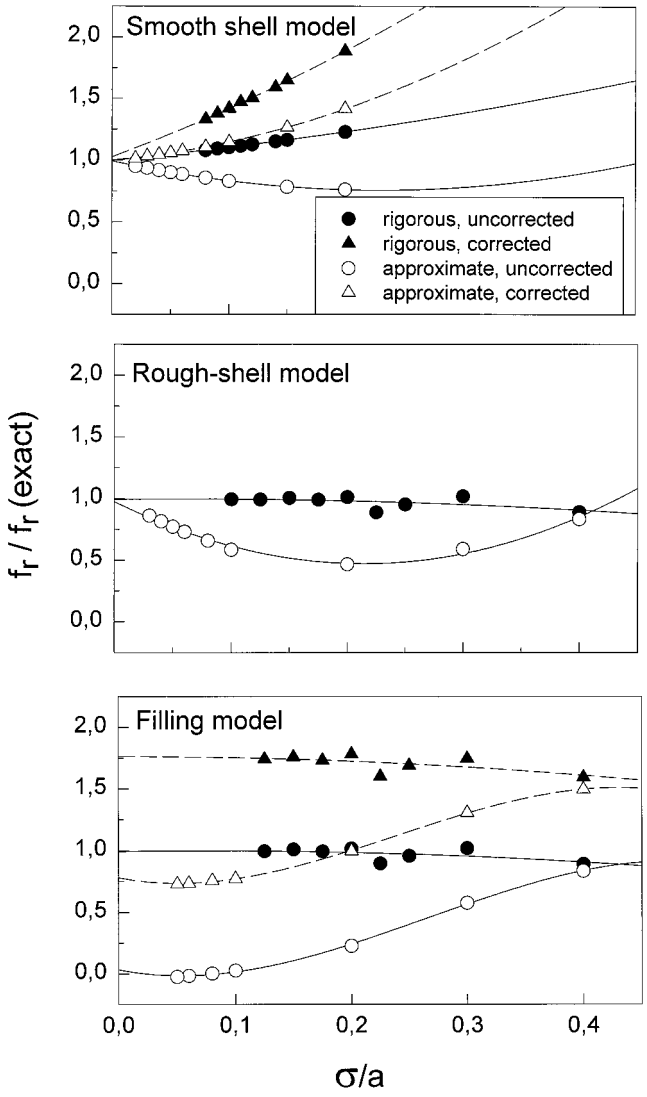

FIGURE 5 Ratios between the calculated translation friction coefficient of the model, f_r, and the exact value of the sphere.

shielded and cannot contribute to the hydrodynamic properties because they do not experience friction. When rigorous hydrodynamic interaction is used, the shielding effect is accounted for properly [see García de la Torre and Bloomfield (1977a) and Schmitz (1977)] and internal beads do not contribute. Therefore, the inclusion of internal beads in the filling model is not reflected in the results. However, if the hydrodynamic interaction is described in an approximate fashion, shielding is incomplete and the internal beads provide a nonzero, incorrect contribution that makes the results worse, which is why the approximate methods give erroneous limits for the filling model (see Figs. 4 and 5 (*bottom*)).

The inclusion of volume correction in the filling model adds further errors. It is clear from Fig. 5 (*bottom*) that the results are about twice the exact ones. This can be explained as follows. The f_r^{uncorr} values for shell models, and for the filling model with rigorous hydrodynamics, are already exact without the volume correction, as justified above. The volume of the filling model, V_m is a fraction close to 1 of the volume of the particle, V_p; for the closest-packing construction, the fraction $q = V_m/V_p$ is $q = 0.74$. Then the total result for the corrected coefficient is found to be $f_r = (1 + q)6\eta_0 V_p$, and the ratio to the exact value is $1 + q = 1.74$, with an error of 74%, which coincides very well with that found numerically from Fig. 5 (*bottom*). The same kind of reasoning can be applied to a particle of any shape. Therefore, it is clearly demonstrated that the volume correction is inadequate for filling models.

Numerical work analogous to that for rotation has been done for viscosity, using the rigorous and approximate procedures for the three types of model. The calculated-to-exact ratios follow the same trend as for rotation. In fact, the corresponding curves are very similar to Figs. 4 and 5 and are not reproduced here. In summary, the effects of modeling procedure, hydrodynamic treatment, and volume correction are the same as for rotational diffusion.

The conclusions from this study of the spherical particle will be listed and summarized along with those from other

models at the end of this paper. We simply remark that the use of filling models should be avoided and that the volume correction is unnecessary for shells. Thus, both strategies will be discarded in the study of the following models.

Dimer

A simple model for which nearly exact, theoretical results are available is the dimer, which is composed of two touching spheres. The most interesting situation is when the two spheres are of the same size; because this is when the difference in hydrodynamic behavior from that of a spherical particle is greatest.

For the dimer of identical spheres, practically exact results are available for translational coefficients (Swanson et al., 1978; Goldman et al., 1966), rotational coefficients (Davis, 1969), and intrinsic viscosity (Wakiya, 1971; Brenner and O'Neil, 1972). For translation and rotation, both the coefficients associated to the center-to-center line (parallel) and a perpendicular axes are available. The overall translational coefficient is $f_t = 1/(1/f_t^{\parallel} + 2/f_t^{\perp})$, and an analogous expression gives the rotational coefficient f_r, which is related to the mean harmonic relaxation time. We have applied our diverse modeling and computational strategies to the dimer, using the various strategies, including the smooth shell model depicted in Fig. 6. The results for the various hydrodynamic properties are listed in Table 1.

In bead modeling, the volume correction seems to improve the rotational calculation, especially rotation along the center-to-center axis. However, the performance is best, with results extremely close to the exact ones, when the cubic substitution is used. With shell models, the results that we obtain with the smooth-shell and rigorous calculations are excellent, with deviations from the exact ones of about 1% for most properties.

If the shell model is calculated with the approximate hydrodynamics, the results for translation, parallel rotation, and intrinsic viscosity show departures of about 5% from the exact results. These departures are larger than the uncertainties associated to the extrapolations, which indicates that the approximate methods introduce some errors, albeit not large, in this case.

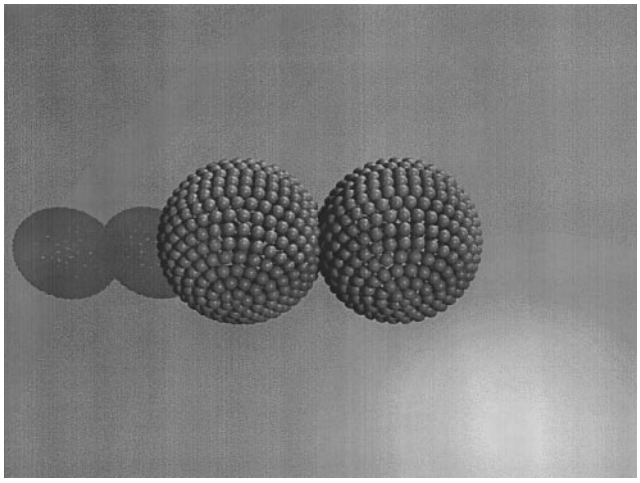

FIGURE 6 Smooth-shell model for a dimer of identical spheres.

Ellipsoids

The hydrodynamic properties of revolution ellipsoids, with semiaxes b, b, and a, and axial ratio $p = a/b$ are known from exact formulas (Perrin, 1936; Simha, 1940). The ellipsoid has therefore been used since the earliest studies (Bloomfield et al., 1967a; Filson and Bloomfield, 1967; García de la Torre and Bloomfield, 1977a, 1978) as a benchmark for testing modeling and computational strategies for nonspherical particles. Our main purpose now is to test the shell modeling procedures, although, for the sake of completeness, we will also summarize previous results for bead models.

Bead modeling of prolate ellipsoids has been described in detail in a series of publications. For a prolate ellipsoid, the bead models consists of a string of colinear, touching beads, with sizes decreasing from the center toward the ends; the beads are inwardly tangent to the surface of the ellipsoid (Bloomfield et al., 1967a). Using the rigorous hydrodynamics, it was shown that the properties of long prolate ellipsoids were accurately predicted for a volume-equalized bead model (García de la Torre and Bloomfield, 1977a, 1978). This illustrates one of the key criteria for bead modeling: for elongated shapes, the bead model must reproduce both the length and the volume of the particle. In contrast, for p close to 1, the models failed to predict rotational coefficients and intrinsic viscosity. More recently, it has been shown that the introduction of the volume corrections (Eq. 39–41) removes this deficiency and gives a reasonably good prediction of the properties over the whole range of axial ratios. For more details, see our recent publication on the volume correction (García de la Torre and Carrasco, 1998). In contrast, bead models of ellipsoids have also been used to test the approximate hydrodynamics with worse results: the rotational coefficients and the intrinsic viscosity for high p are in error by 15–25% (García de la Torre and Bloomfield, 1978; García de la Torre et al., 1987).

In the present study, we have constructed both smooth and rough shell models for ellipsoids, examples of which are displayed in Fig. 3. We first consider the results for translational diffusion coefficient, f_t. In Fig. 7 *A* we note that, in all four cases, the deviations oscillate about zero, and the average absolute deviation is smaller than 2%. The performance of the smooth shell model with rigorous hydrodynamics is particularly excellent with the small fluctuations most probably attributable to the extrapolations. We therefore conclude that the shell-modeling predicts the f_t of ellipsoids correctly, even with approximate hydrodynamics. A similar analysis of the intrinsic viscosity $[\eta]$ result leads to the results displayed in Fig. 7 *B*. The errors from rigorous

TABLE 1 Intrinsic viscosity and rotational and translational coefficients for a dimer

Modeling Strategy	Hydrodynamic Calculation	Volume Correction	$f^{\parallel}_{t,2}/f^{\parallel}_{t,1}$	$f^{\perp}_{t,2}/f^{\perp}_{t,1}$	$f_{t,2}/f_{t,1}$	$f^{\parallel}_{r,2}/f^{\parallel}_{r,1}$	$f^{\perp}_{r,2}/f^{\perp}_{r,1}$	$f_{r,2}/f_{r,1}$	$[\eta]_2/[\eta]_1$
Bead	Rigorous	NO	1.230	1.392	1.333	0.00	2.67	0.00	0.64
Bead	Rigorous	YES	1.230	1.392	1.333	2.00	4.67	3.23	1.64
Bead cubic substitution	Rigorous	NO	1.276	1.458	1.392	1.77	3.79	2.75	1.34
Smooth shell	Rigorous	NO	1.286	1.446	1.388	1.83	3.75	2.78	1.37
Smooth shell	Approximate	NO	—	—	1.336	1.84	3.75	2.81	1.30
Exact	—	—	1.290	1.449	1.392	1.78	3.76	2.74	1.39

hydrodynamics still fluctuate about zero, although their absolute values are larger than those obtained for f_t, with an average of 2–3%. In contrast, the results from the approximate formula show a systematic error of close to 10%. We conclude that the rigorous method gives the correct $[\eta]$ for the shell models of ellipsoids, whereas the approximate double sum does not. It is interesting to note that the error of the approximate method for the shell model of the ellipsoids is very similar to that found earlier with beads models (García de la Torre and Bloomfield, 1978).

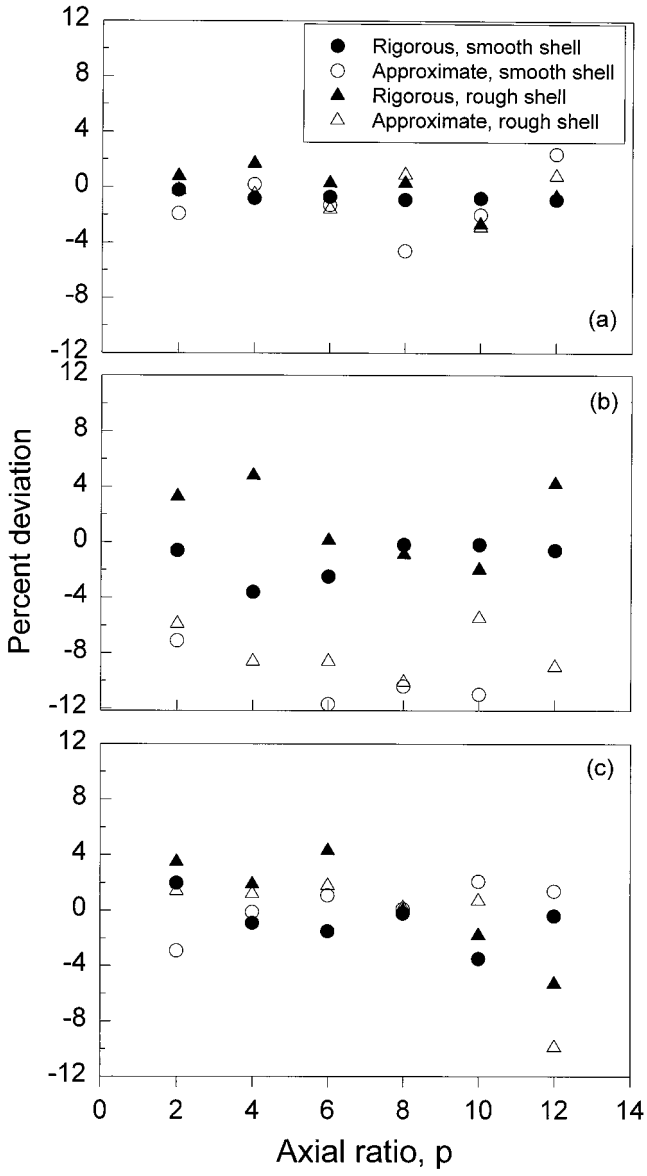

FIGURE 7 Percent deviation from the exact values of the results from shell model calculations for ellipsoids. Cases with smooth and rough models, and with rigorous and approximate hydrodynamics. (*A*) Translation friction coefficient. (*B*) Intrinsic viscosity. (*C*) Rotational friction coefficient.

As described in subsection Basic theory: Rigorous methods, the rotational dynamics can be characterized in terms of different quantities. For the presentation of data in Fig. 7 *C*, we have chosen the mean rotational friction coefficient (Eq. 31), which is related to the harmonic mean of the relaxation times (Eq. 12). The errors for f_r in the four cases show no systematic trend. The fluctuation due to extrapolation and model imperfections are larger than those for the other two properties although the average error is around zero. Similar plots (not shown) for other rotational quantities show the same situation, which leads us to conclude that the rotational quantities of ellipsoids are predicted correctly with both rigorous and approximate hydrodynamics. This is in agreement with a result with bead models of a rod, for which the rotational coefficient from the approximate method is correct at high aspect ratio (García de la Torre et al., 1987).

OLIGOMERIC STRUCTURES

Oligomeric structures, in which a few elements are arrayed in a polygonal or polyhedral array, are typical examples of bead modeling (Bloomfield and Filson, 1968; García de la Torre and Bloomfield, 1978; García Bernal and García de la Torre, 1981).

For more compact structures, anomalies of the type that motivated the volume correction have been detected. Before the proposal of the volume correction, García Bernal and García de la Torre (1981) used the cubic substitution for these structures and tabulated results of various properties for a number of geometries, which have been widely used (García de la Torre, 1989). When the volume correction was applied to these structures (García de la Torre and Carrasco, 1998) the results were not entirely satisfactory.

In the present work, prior analyses of the oligomeric structures are complemented with shell-model calculations. Although no exact results are available for these structures, among the various strategies, the shell model and the cubic substitution are probably the most accurate. Because the

shell model results still include some imperfections due to extrapolation, we chose as the reference values in this case those obtained for bead models with cubic substitution. To illustrate the performance of the various methods, we just consider a set of hexamers with different geometries and therefore varying compactness, from a linear string to an octahedron. The results for translation, rotation, and viscosity are given in Table 2. It is well clear that the results from the cubic substitution are almost identical to those from the shell model with rigorous hydrodynamics, and we expect that both, in turn, should be nearly exact. The plain (unsubstituted) bead model gives reasonable results for translation, but shows the well-known failure for rotation and viscosity.

Finally, it is interesting to note that, unlike in the case of the sphere or the ellipsoid, the shell model with approximate hydrodynamics gives bad results in the present case. The spherical particle and the octahedral array of spheres have in common the fact of being isometric; tensors representing physical quantities, like the inertia and friction tensors, have three identical eigenvalues. In some regards the two particles have an aspect ratio of unity. However, the shell model with approximate calculation performs well for the sphere but badly for the octahedral array, perhaps because the sphere and the ellipsoid are simple convex bodies, whereas the oligomeric arrays are geometrically more complex, with holes, convex, and concave parts, etc. Such structural features may influence the performance of the shell model with approximate hydrodynamics more than the overall aspect ratio of the particle.

COMPUTER PROGRAMS

The computer program used to produce the objects in Figs. 2 and 3 is the POLYRAY raytracing software, which is of public domain and can be found in the Internet (see, for instance, http://ftp.tu-clausthal.de/pub/TEXT/mirror/povray/polyray).

The calculation of the basic properties (s, D_t, $[\eta]$, the five τ, etc.) using rigorous hydrodynamics, the previously published HYDRO (García de la Torre et al., 1994) (file: hydrox_x.f; where _x denotes the version number) computer program can be used. During the course of this work we have developed various computer program that are described below.

APPROX (file: hydosu_x.f) is a subroutine that implements all the approximate double-sum formulas. Its input data and the computed quantities are the same as those for HYDRO. The use of the two subroutines is very similar. Based on the experience obtained in the present work concerning the volume correction, which was an integral part of the calculations with older versions of HYDRO, we now leave that correction as a user-decided option.

The most novel software pieces are several subroutines intended to build shell models and the intermediate filling models used for scattering-related properties. For an arbitrarily shaped particle, the intermediate filling model is built by RFILL (file: rgfill_x.f), from which one can calculate R_g and the scattering-related properties using CAFILL (file: cafill_x.f). The rough shell model to be used for hydrodynamics is then built by using subroutine RSHELL (file: rshell_x.f). We have even designed a program, SHELLSYM (file: shesym_x.f) that constructs smooth shell models for the particular (although frequent and/or useful) case of particles composed of axially symmetric blocks (spheres, cylinders, or ellipsoids). Finally, we have a subroutine, SH_RG_EX (file: extrap_x.for) which drives a model-building subroutine along with HYDRO or APPROX, to perform calculations with variable σ and extrapolate to the shell model limit.

All those pieces of software are complemented by another subroutine, SOLPRO, which takes the bead model data and the basic properties calculated by HYDRO, and calculates a number of more complex solution properties, both dynamic quantities such as nuclear magnetic resonance

TABLE 2 Results for the hydrodynamic properties of hexameric arrays

Strategy	Hexagon	Trigonal Prism	Octahedron	Linear String
$f_t(6)/f_t(1)$				
Cubic substitution	1.13	1.05	1.02	1.29
Bead model	1.07 (6)	0.96 (8)	0.93 (9)	1.26 (2)
Shell model, rigorous	1.13 (0)	1.04 (0)	1.02 (1)	1.30 (−1)
Shell model, approximate	1.06 (6)	0.94 (11)	0.89 (13)	1.23 (5)
$f_r(6)/f_r(1)$				
Cubic substitution	2.23	1.61	1.47	1.96
Bead model	2.67 (−20)	2.11 (−31)	2.22 (−51)	2.42 (−23)
Shell model, rigorous	2.21 (1)	1.60 (1)	1.46 (1)	2.01 (3)
Shell model, approximate	2.05 (8)	1.52 (6)	1.26 (14)	1.95 (1)
$[\eta](6)/[\eta](1)$				
Cubic substitution	15.3	11.6	10.9	28.9
Bead model	18.9 (−24)	16.5 (−42)	15.9 (−46)	30.9 (−7)
Shell model, rigorous	15.6 (2)	11.5 (1)	11.1 (1)	28.9 (0)
Shell model, approximate	13.1 (14)	10.5 (9)	9.8 (10)	24.5 (15)

Results of the hexamers (6) are normalized to those of the monomer, i.e., of the constituting spheres.
The numbers in parentheses are the percent deviation from the cubic substitution results.

relaxation, transient electric birefringence, etc.) as well as other equilibrium properties, including scattering form factor, covolume, and many dimensionless combinations of solution properties. More details on SOLPRO can be found elsewhere (García de la Torre et al., 1997, 1999).

All these software modules are of public domain and can be downloaded from the Internet from our web site, http://leonardo.fcu.um.es/macromol.

CONCLUSIONS

Summarizing the findings of the various parts of the present study, the main conclusions are:

- Bead models in the strict sense (with few elements) provide a convenient way of calculating hydrodynamic properties. The volume correction provides an easy, inexpensive way of correcting the Kirkwood–Riseman treatment of rotation and viscosity.
- The hydrodynamic properties calculated from models of the filling type can be extremely erroneous, particularly when the volume correction is applied for rotation and viscosity, and when the properties are calculated from the approximate, double-sum formulas.
- The volume correction is not necessary for shell models.
- Shell-model calculations with the approximate double-sum formulas give the exact results for a spherical particle. Thus the approximate methods (APPROX) with shell-modeling is potentially useful for nearly spherical particles, such as some globular proteins. Nonetheless, a separate calculation with the rigorous procedures (HYDRO) should also be made, and the properties calculated by double extrapolation, as in Fig. 4 *A* and *B* and 5 *A* and *B*.

These conclusions will provide a useful guidance for refined or novel calculation of properties, by application of the different model strategies, for a variety of structures ranging from the regular shapes of the oligomeric, multisubunit proteins to the oddly shaped structures of bacteriophage.

We acknowledge support by grant PB96-1106 from the Dirección General de Enseñanza Superior. B.C. is the recipient of a predoctoral fellowship from the same source.

REFERENCES

Abe, F., Y. Einaga, and H. Yamakawa. 1991. Intrinsic viscosity of oligo- and poly-isobutylenes. Treatments of negative intrinsic viscosities. *Macromolecules.* 24:4423–4428.

Allison, S. A., and J. A. McCammon. 1984. Transport properties of rigid and flexible macromolecules by Brownian dynamic simulation. *Biopolymers.* 23:167–187.

Bianchi, U., and a. Peterlin. 1968. Intrinsic viscosity of polymers of low molecular weight. *J. Polym. Sci. Part A-2.* 6:1759–1772.

Bloomfield, V. A. 1966. The structure of bovine serum albumin at low pH. *Biochemistry.* 5:684–689.

Bloomfield, V. A., W. O. Dalton, and K. E. V. Holde. 1967a. Frictional coefficients of multisubunit structures. I. Theory. *Biopolymers.* 5:135–148.

Bloomfield, V. A., W. O. Dalton, and K. E. V. Holde. 1967b. Frictional coefficients of multisubunit structures. II. Application to proteins and viruses. *Biopolymers.* 5:149–159.

Bloomfield, V. A., and D. P. Filson. 1968. Shell model calculations of translational and rotational frictional coefficients. *J. Polym. Sci. Part C.* 25:73–83.

Brenner, H., and M. E. O'Neil. 1972. On the Stokes resistance of multiparticle system in a linear shear field. *Chem. Eng. Sci.* 27:1421–1439.

Davis, M. H. 1969. The slow translational and rotation of two unequal spheres in a viscous flow. *Chem. Eng. Sci.* 24:1769–1776.

Filson, D. P., and V. A. Bloomfield. 1967. Shell model calculations of rotational diffusion coefficients. *Biochemistry.* 6:1650–1658.

García Bernal, J. M., and J. García de la Torre. 1980. Transport properties and hydrodynamic centers of rigid macromolecules with arbitrary shape. *Biopolymers.* 19:751–766.

García Bernal, J. M., and J. García de la Torre. 1981. Transport properties of oligomeric subunit structures. *Biopolymers.* 20:129–139.

García de la Torre, J. 1981. Rotational diffusion coefficients. *In* Molecular Electro-Optics. S. Krause, editor. Plenum Press, New York. 75–103.

García de la Torre, J. 1989. Hydrodynamic properties of macromolecular assemblies. *In* Dynamic Properties of Macromolecular Assemblies. S. E. Harding and A. J. Row, editors. The Royal Society of Chemistry, Cambridge University Press, Cambridge, U.K. 3–31.

García de la Torre, J. 1992. Sedimentation coefficients of complex biological particles. *In* Analytical Centrifugation in Polymer Science and Biochemistry, S. E. Harding, A. J. Rowe, and J. C. Horton, editors. The Royal Society of Chemistry, Cambridge University Press, Cambridge, U.K. 333–345.

García de la Torre, J., and V. A. Bloomfield. 1977a. Hydrodynamic properties of macromolecular complexes. I. Translation. *Biopolymers.* 16:1747–1763.

García de la Torre, J., and V. A. Bloomfield. 1977b. Hydrodynamic properties of macromolecular complexes. II. Rotation. *Biopolymers.* 16:1765–1778.

García de la Torre, J., and V. A. Bloomfield. 1977c. Hydrodynamic properties of macromolecular complexes. III. Bacterial viruses. *Biopolymers.* 16:1779–1793.

García de la Torre, J., and V. A. Bloomfield. 1978. Hydrodynamic properties of macromolecular complexes. IV. Intrinsic viscosity theory with applications to once-broken rods and multisubunit proteins. *Biopolymers.* 17:1605–1627.

García de la Torre, J., and V. A. Bloomfield. 1981. Hydrodynamic properties of complex, rigid, biological macromolecules. Theory and applications. *Quart. Rev. Biophys.* 14:81–139.

García de la Torre, J., and B. Carrasco. 1998. Intrinsic viscosity and rotational diffusion of bead models for rigid particles. *Eur. Biophys. J.* 27:549–557.

García de la Torre, J., B. Carrasco, and S. E. Harding. 1997. SOLPRO: Theory and computer program for the prediction of SOLution PROperties of rigid macromolecules and bioparticles. *Eur. Biophys. J.* 25: 361–372.

García de la Torre, J., S. E. Harding, and B. Carrasco. 1999. Calculation of NMR relaxation, covolume and scattering-related properties of bead models using the solpro computer program. *Eur. Biophys. J.* 28: 119–132.

García de la Torre, J., M. C. López Martínez, and J. J. García Molina. 1987. Approximate methods for calculating rotational diffusion constants of rigid macromolecules. *Macromolecules.* 20:661–666.

García de la Torre, J., M. C. López Martínez, M. M. Tirado, and J. J. Freire. 1983. Approximate methods for calculating hydrodynamic properties of macromolecules in dilute solution. Theory and application to rigid structures. *Macromolecules.* 16:1121–1127.

García de la Torre, J., S. Navarro, M. C. López Martínez, F. G. Díaz, and J. J. López Cascales. 1994. HYDRO: a computer software for the prediction of hydrodynamic properties of macromolecules. *Biophys. J.* 67:530–531.

García de la Torre, J., and V. Rodes. 1983. Effects from bead size and hydrodynamic interactions on the translational and rotational coefficients of macromolecular bead models. *J. Chem. Phys.* 79:2454–2460.

Goldman, A. J., R. G. Cox, and H. Brenner. 1966. The slow motion of two identical arbitrarily oriented spheres through a viscous fluid. *Chem. Eng. Sci.* 21:1151–1170.

Hagerman, P. I., and B. H. Zimm. 1982. Monte-Carlo approach to the analysis of the rotational diffusion of wormlike chains. *Biopolymers.* 20:1481–1502.

Harvey, S. H., and J. García de la Torre. 1980. Coordinate systems for modelling the hydrodynamic resistance and diffusion coefficients of irregularly shaped rigid macromolecules. *Macromolecules.* 13:960–964.

Hearst, J. E. 1962. Rotatory diffusion constants of stiff-chain macromolecules. *J. Chem. Phys.* 38:1062–1065.

Kirkwood, J. G. 1954. The general theory of irreversible processes in solutions of macromolecules. *J. Polym. Sci.* 12:1–14.

Kirkwood, J. G., and J. Riseman. 1948. The intrinsic viscosities and diffusion constants of flexible macromolecules in solution. *J. Chem. Phys.* 16:565–573.

McCammon, J. A. 1976. Frictional properties of nonspherical multisubunits structures. Application to tubules and cylinders. *Biopolymers.* 15:1397–1408.

Muller, J. J. 1983. Calculation of scattering curves for macromolecular in solution and comparison with results of methods using effective atomic scattering factors. *J. Appl. Cryst.* 16:78–82.

Muller, J. J., O. Glatter, D. Zirwer, and G. Damaschun. 1983a. Calculation of small-angle X-ray and neutron scattering curves and of translational friction coefficients on the common basis of finite elements. *Studia Biophysica.* 93:39–46.

Muller, J. J., D. Zirwer, G. Damaschun, H. Welfle, K. Gast, and P. Plietz. 1983b. The translational frictional coefficients of rape seed 11S globulin, tRNA and ribosomal 5S RNA. Calculations on the basis of finite elements. *Studia Biophysica.* 93:39–46.

Nakajima, H., and Y. Wada. 1977. A general method for the evaluation of diffusion constant, dilute-solution viscoelasticity and the complex dielectric constant of a rigid macromolecule with an arbitrary configuration. I. *Biopolymers.* 16:875–893.

Navarro, S., M. C. López Martínez, and J. García de la Torre. 1995. Relaxation times in transient electric birefringence and electric field light scattering of flexible polymer chains. *J. Chem. Phys.* 103: 7631–7639.

Pavlov, M. Y., and B. A. Fedorov. 1983. Improved technique for calculating X-ray scattering intensity of biopolymers in solution: evaluation of the form, volume, and surface of a particle. *Biopolymers.* 22: 1507–1522.

Pavlov, M. Y., M. A. Sinev, A. A. Timchenko, and O. B. Ptitsyn. 1986. A study of apo- and holo-forms of horse liver alcohol dehydrogenase in solution by diffuse X-ray scattering. *Biopolymers.* 25:1385–1397.

Perrin, F. 1936. Mouvement Brownien d'un ellipsoide. I. Translation et diffusion de molécules ellipsoidales. *J. Phys. Radium.* 7:1–11.

Riseman, J., and J. G. Kirkwood. 1950. The intrinsic viscosity, translational and rotatory diffusion constants of rod-like macromolecules in solution. *J. Chem. Phys.* 18:512–516.

Riseman, J., and J. G. Kirkwood. 1956. The statistical mechanical theory of irreversible processes in solutions of macromolecules. *In* Rheology–Theory and Applications. Vol. 1, Chap. 13, Academic Press, New York. 495.

Rotne, J., and S. Prager. 1969. Variational treatment of hydrodynamic interaction on polymers. *J. Chem. Phys.* 50:4831–4837.

Schmitz, K. S. 1977. Hydrodynamic shielding of spherical subunits in macromolecular complexes. *Biopolymers.* 16:2635–2640.

Simha, R. 1940. The influence of Brownian movement on the viscosity of solutions. *J. Phys. Chem.* 44:25–34.

Swanson, E., D. C. Teller, and C. De Haen. 1978. The low Reynold number translational friction of ellipsoid, cylinders, dumbbells, and hollow spherical caps. Numerical testing of the validity of the modified Oseen tensor in computing the friction of objects modeled as beads on a shell. *J. Chem. Phys.* 68:5097–5102.

Teller, D. C., E. Swanson, and C. de Häen. 1979. The translational friction coefficient of proteins. *Methods Enzymol.* 61:103–124.

Tirado, M. M., and J. García de la Torre. 1979. Translational friction coefficients of rigid, symmetric top macromolecules. *J. Chem. Phys.* 71:2581–2587.

Tirado, M. M., and J. García de la Torre. 1980. Rotational dynamics of rigid, symmetric top macromolecules. *J. Chem. Phys.* 73:1968–1993.

Tirado, M. M., M. C. López Martínez, and J. García de la Torre. 1984. Comparison of theories for the translational and rotational diffusion coefficients of rodlike Monte Carlo. Application to short rodlike cylinders. *J. Chem. Phys.* 81:2047–2052.

Tsuda, K. 1970a. Hydrodynamic properties of rigid complex molecules. *Polym. J.* 1:616–631.

Tsuda, K. 1970b. Intrinsic viscosity of rigid complex molecules. *Rheol. Acta.* 9:509–516.

Wakiya, S. 1971. Slow motion in shear flow of a doublet of two spheres in contact. *J. Phys. Soc. Jpn.* 31:1581–1587.

Wilson, R. W., and V. A. Bloomfield. 1979. Hydrodynamic properties of macromolecular complexes. V. Improved calculation of rotational diffusion coefficient and intrinsic viscosity. *Biopolymers.* 18:1205–1211.

Yamakawa, H. 1970. Transport properties of polymer chains in dilute solutions. Hydrodynamic interaction. *J. Chem. Phys.* 53:436–443.

Yoshizaki, T., I. Nita, and H. Yamakawa. 1988. Transport coefficients of helical wormlike chains. IV. Intrinsic viscosity of the touched-bead model. *Macromolecules.* 21:165–171.